

# The involvement of endoplasmic reticulum stress in bile acid-induced hepatocellular injury

Tetsuo Adachi,\* Tomoyuki Kaminaga, Hiroyuki Yasuda, Tetsuro Kamiya and Hirokazu Hara

Laboratory of Clinical Pharmaceutics, Gifu Pharmaceutical University, 1-25-4 Daigaku-nishi, Gifu 501-1196, Japan

(Received 31 May, 2013; Accepted 25 September, 2013; Published online 27 December, 2013)

**Secondary bile acids produced by enteric bacteria accumulate to high levels in the enterohepatic circulation and may contribute to the pathogenesis of hepatocellular injury. Relative hydrophobicity has been suggested to be an important determinant of the biological properties of these compounds, although the mechanism by which bile acids induce pathogenesis is not fully understood. On the other hand, endoplasmic reticulum stress has been shown to be involved in the induction and development of various pathogenic conditions. In this report, we demonstrated that the intensities of cytotoxicity and endoplasmic reticulum stress in HepG2 cells triggered by the bile acids tested were largely dependent on their hydrophobicity. The activation of caspase-3 and DNA fragmentation by treatment with chenodeoxycholic acid showed the contribution of apoptosis to cytotoxicity. Increases in intracellular calcium levels and the generation of reactive oxygen species stimulated by treatment with chenodeoxycholic acid contributed to endoplasmic reticulum stress. Bile acids also induced transforming growth factor- $\beta$ , a potent profibrogenic factor, which is known to induce hepatocyte apoptosis and ultimately liver fibrosis. In conclusion, our study demonstrated that bile acids induced endoplasmic reticulum stress, which in turn stimulated apoptosis in HepG2 cells, in a hydrophobicity-dependent manner.**

**Key Words:** bile acid, endoplasmic reticulum stress, apoptosis, transforming growth factor- $\beta$ , hydrophobicity

Bile acids are amphipathic detergents necessary for the digestion and absorption of fat-soluble nutrients. After their synthesis by the liver and excretion into the digestive tract, bile acids are metabolized by enteric bacteria mainly through deconjugation, oxidation, and epimerization to produce secondary bile acids.<sup>(1,2)</sup> These secondary bile acids are deoxycholic acid (DCA) and lithocholic acid (LCA), which are the 7-dehydroxylation products of cholic acid (CA) and chenodeoxycholic acid (CDCA), respectively. A few species of intestinal bacteria have been shown to be able to epimerize CDCA to ursodeoxycholic acid (UDCA).<sup>(1)</sup> Most bile acids are absorbed from the intestine and returned to the liver, which is known as enterohepatic circulation.

Endoplasmic reticulum (ER) stress has recently been shown to be involved in the induction and development of various diseases including liver diseases.<sup>(3,4)</sup> The ER is the intracellular organelle responsible for the synthesis, folding, and maturation of proteins as well as the storage and release of intracellular calcium ( $\text{Ca}^{2+}$ ). An intricate homeostatic adaptive response to the accumulation of unfolded protein molecules and/or the depletion of intracellular  $\text{Ca}^{2+}$  leading to the ER stress response has been referred to as the unfolded protein response (UPR).<sup>(4)</sup> This response was shown to improve the ability of protein folding by inducing an ER resident chaperone such as glucose-regulated protein 78 (GRP78).<sup>(5)</sup> However, when activation of the UPR fails to promote cell survival, the cell is broken down by the proapoptotic ER stress response pathway. C/EBP homologous protein (CHOP) is a

transcriptional regulator induced by ER stress and is also a key factor in the ER stress-mediated apoptosis pathway.<sup>(6)</sup> Increases in GRP78 and/or CHOP were shown to be good markers of the presence of ER stress.

Plasma concentrations of bile acids are commonly elevated in patients with hepatobiliary diseases,<sup>(7,8)</sup> and high concentrations of bile acids have been shown to result in hepatic inflammatory conditions such as that during cholestasis<sup>(9)</sup> and eventually cirrhosis.<sup>(10)</sup> Although the mechanism by which bile acids induce hepatic inflammation is not fully understood, relative hydrophobicity has been suggested to be an important determinant of the biological properties of these compounds.<sup>(11)</sup> It has been hypothesized that bile acids with increased hydrophobicity may have a greater capacity to perturb the cell membrane and/or pass through the membrane and interact with intracellular molecules.<sup>(12)</sup>

In this study, we investigated the contribution of bile acids to hepatocellular injury accompanied by ER stress, and the relationship between the hydrophobicity of these bile salts and the intensity of cytotoxicity and ER stress induced. The participation of intracellular  $\text{Ca}^{2+}$  and reactive oxygen species (ROS) was also investigated.

## Materials and Methods

**Cell culture.** HepG2 cells were grown to confluence in a 35-mm or 60-mm culture dish or in a 96-well microplate in Dulbecco's modified Eagle's medium (DMEM) supplemented with 10% fetal calf serum (FCS), 100 units/ml penicillin, and 100  $\mu\text{g}/\text{ml}$  streptomycin under an atmosphere of 5%  $\text{CO}_2/95\%$  air at 37°C.

**Reagents.** CDCA, tauroursodeoxycholic acid (TUDCA), glycochenodeoxycholic acid (GCDCA), and 1,2-bis(2-amino-phenoxy)ethane-*N,N,N',N'*-tetraacetic acid tetraacetoxymethyl ester (BAPTA-AM) were purchased from Nacalai Tesque, Kyoto, Japan. UDCA and CA were purchased from Tokyo Chemical Industry, Tokyo, Japan. DCA and LCA were purchased from Wako Pure Chem. Ind., Ltd., Osaka, Japan. Diphenylethylidene diisopropyl carbodiimide (DPI) and *N*<sup>G</sup>-nitro-L-arginine methyl ester (L-NAME) were purchased from Enzo Life Sciences (Farmingdale, NY). The structure of the above unconjugated bile acids and their lipophilicity index ( $R_{\text{MW}}$ )<sup>(13)</sup> are shown in Fig. 1.

**Measurement of cell viability.** A 3-(4,5-di-methylthiazol-2-yl)-2,5-diphenyltetrazolium bromide (MTT) assay was used to estimate the cytotoxicity of the bile acids. Following the treatment of HepG2 cells with bile acids in a 96-well microplate, the culture medium was aspirated, and cells were added to 100  $\mu\text{l}$  of 10% FCS-DMEM containing 0.5 mg/ml MTT (Chemicon Int. Inc., Temecula, CA). They were then incubated at 37°C for 2 h in a humidified atmosphere of 5%  $\text{CO}_2/95\%$  air. After incubation,

\*To whom correspondence should be addressed.  
E-mail: adachi@gifu-pu.ac.jp

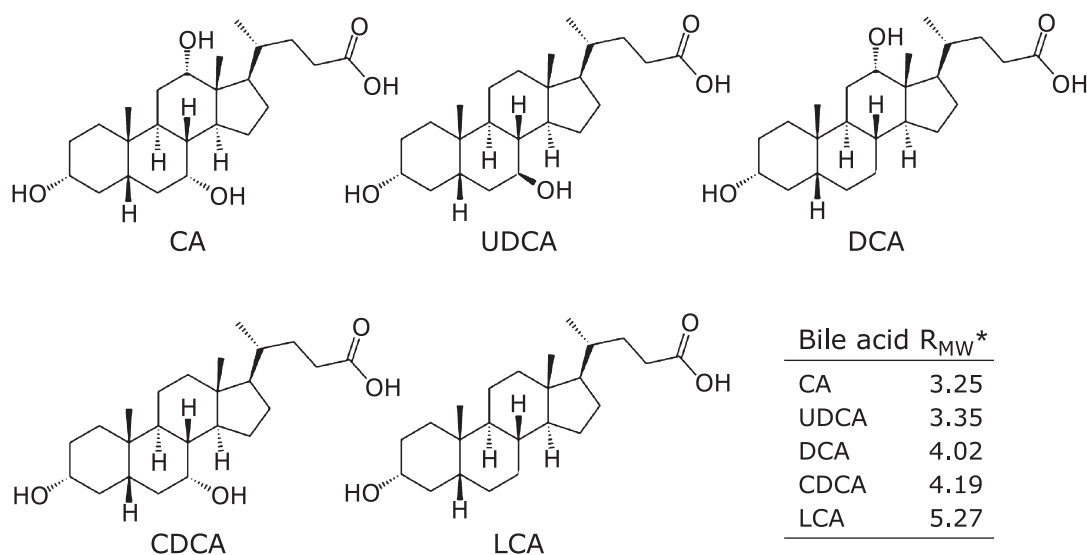


**Fig. 1.** Molecular structures of unconjugated bile acids and their lipophilicities. \*The lipophilicity index ( $R_{MW}$ ) is cited as the values described in Ref. 13.

cells were added to 100  $\mu$ l isopropanol containing 0.04 N HCl and were then mixed thoroughly to dissolve MTT formazan. MTT formazan was measured at 595 nm with a reference wavelength of 655 nm.

**Polymerase chain reaction analysis.** Cells were cultured and treated in a 35-mm culture dish. After the treatment, cells were washed with cold phosphate-buffered saline (PBS) and total RNA was extracted from cells with TRIzol reagent (Invitrogen, Carlsbad, CA). The preparation of cDNA was performed by the method described in our previous report<sup>(14)</sup> and real-time polymerase chain reaction (PCR) was carried out by an intercalater method with SYBR Premix Ex Taq (Takara Bio Inc., Otsu, Japan) according to the manufacturer's directions. The primers for real-time PCR were as follows: GRP78, sense 5'-GAA CAT CCT GGT GTT TGA CC-3'; antisense 5'-CCC AGA TGA GTA TCT CCA TT-3'; CHOP, sense 5'-CTC TGG CTT GGC TGA CTG A-3'; antisense 5'-GCT CTG GGA GGT GCT TGT-3'; transforming growth factor- $\beta$  (TGF- $\beta$ ), sense 5'-TGA GGC CGA CTA CTA CGC CA-3'; antisense 5'-CCG AGA AGC GGT ACC TGA AC-3'; glyceraldehyde-3-phosphate dehydrogenase (GAPDH), sense 5'-TGA CTT CAA CAG CGA CAC CC-3'; antisense 5'-TCC ACC ACC CTG TTG CTG TA-3'. Each mRNA level was normalized relative to the GAPDH mRNA level in each sample.

Reverse transcriptional-polymerase chain reaction (RT-PCR) of NADPH oxidase 4 (NOX4) was performed by the method described in our previous report<sup>(14)</sup> with primers of sense 5'-CTC AGC GGA ATC AAT CAG CTG TG-3' and antisense 5'-AGA GGA ACA CGA CAA TCA GCC TTA G-3'. We ascertained that there was a linear correlation between the amounts of PCR products and template cDNA under our PCR conditions. Aliquots of the PCR mixture were separated on a 2% agarose gel and stained with ethidium bromide. Densitometric analysis of the PCR products was performed with Multi Gauge ver. 3.0 (Fuji Film, Tokyo, Japan).

**Western blotting.** HepG2 cells were cultured and treated with reagents in a 60-mm culture dish. After the treatment, cells were washed with cold PBS, scraped and lysed in 200  $\mu$ l of lysis buffer (20 mM Tris-HCl pH 7.4 containing 1 mM EDTA, 1 mM EGTA, 10 mM NaF, 1 mM Na<sub>2</sub>VO<sub>4</sub>, 20 mM  $\beta$ -glycerophosphate, 1 mM phenylmethylsulfonyl fluoride, 1 mM dithiothreitol (DTT), 2  $\mu$ g/ml leupeptin, and 1% Triton X-100) followed by centrifugation at 17,000  $\times$  g for 5 min. After centrifugation, the protein

concentration of the supernatant was assayed using a protein assay reagent (Bio-Rad Laboratories, Hercules, CA). Extracts containing 20  $\mu$ g of protein were boiled with sample buffer (62.5 mM Tris-HCl pH 6.8 containing 2% sodium dodecylsulfate (SDS), 10% glycerol, 50 mM DTT and 0.01% bromophenol blue) for 5 min and separated by SDS-PAGE on a 12 or 15% (w/v) polyacrylamide gel. After being transferred electrophoretically onto PVDF membranes, nonspecific binding sites were blocked with PBS containing 1% bovine serum albumin. The membranes were subsequently incubated with the respective specific primary antibodies (1:1,000) as follows: anti-human GRP78 rabbit polyclonal antibody and anti-human CHOP rabbit polyclonal antibody (Santa Cruz Biotechnology, Dallas, TX); anti-human TGF- $\beta$ 1 rabbit polyclonal antibody (BioVision, Milpitas, CA). After the membranes had been washed three times with PBS containing 0.1% Tween 20 (PBST), the blots were incubated with the biotin-conjugated goat anti-rabbit IgG antibody (Invitrogen) (1:1,000). After the membranes had been washed three times with PBST, the blots were incubated with ABC reagents (Vector Laboratories, Burlingame, CA) (1:5,000). After the membranes had again been washed with PBST, the bands were detected using SuperSignal<sup>®</sup> West Pico (Thermo Scientific, Rockford, IL), and imaged using an LAS-3000 UV mini (Fuji Film).

**DNA fragmentation.** After the treatment of HepG2 cells with CDCA, cells were washed twice with ice-cold PBS and lysed on ice for 20 min in lysis buffer (10 mM Tris-HCl pH 8.0 containing 10 mM EDTA and 0.5% Triton X-100). The lysates were centrifuged at 13,000  $\times$  g for 10 min. The supernatants were deproteinized by digestion with 200  $\mu$ g/ml proteinase K at 50°C for 30 min, extracted once with an equal volume of phenol:chloroform:isoamylalcohol mixture (25:24:1), and were then precipitated with 2.5 volumes of ethanol in the presence of 0.3 M sodium acetate. After centrifugation at 17,700  $\times$  g for 10 min, the pellet was washed once with 70% ethanol and re-suspended in 20  $\mu$ l of 10 mM Tris-HCl pH 8.0 containing 1 mM EDTA and 10  $\mu$ g/ml RNase. The DNA solution was incubated at 37°C for 1 h, and a 10  $\mu$ l aliquot was separated on 1.5% agarose gel, stained with ethidium bromide, and photographed.

**Assay of caspase-3 activity.** After the treatment of HepG2 cells with CDCA, cells were washed twice with ice-cold PBS and collected by centrifugation at 550  $\times$  g for 10 min. The pellet was lysed on ice for 10 min in lysis buffer. Caspase-3 activity was then

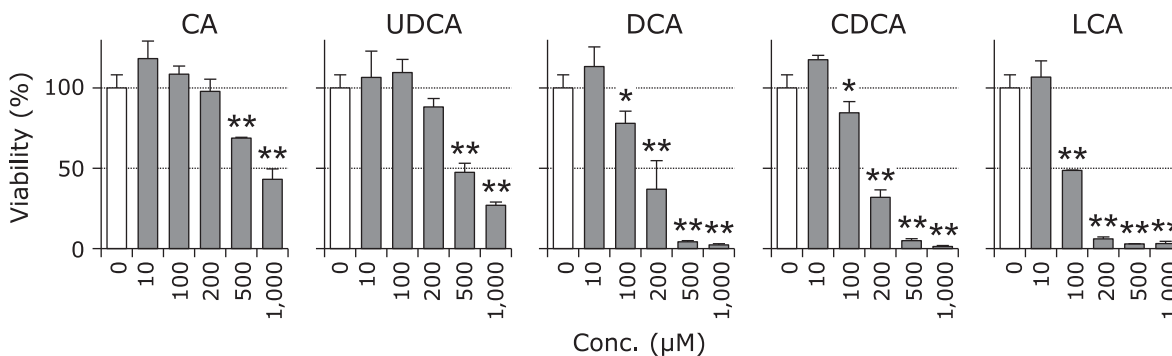


**Fig. 2.** Effect of unconjugated bile acids on HepG2 cell viability. HepG2 cells were treated with the indicated concentrations of unconjugated bile acids such as CA, UDCA, DCA, CDCA, and LCA for 24 h, and cell viability was measured. Data are shown as the mean  $\pm$  SD ( $n = 3$ ). \* $p < 0.05$ , \*\* $p < 0.01$  vs vehicle.

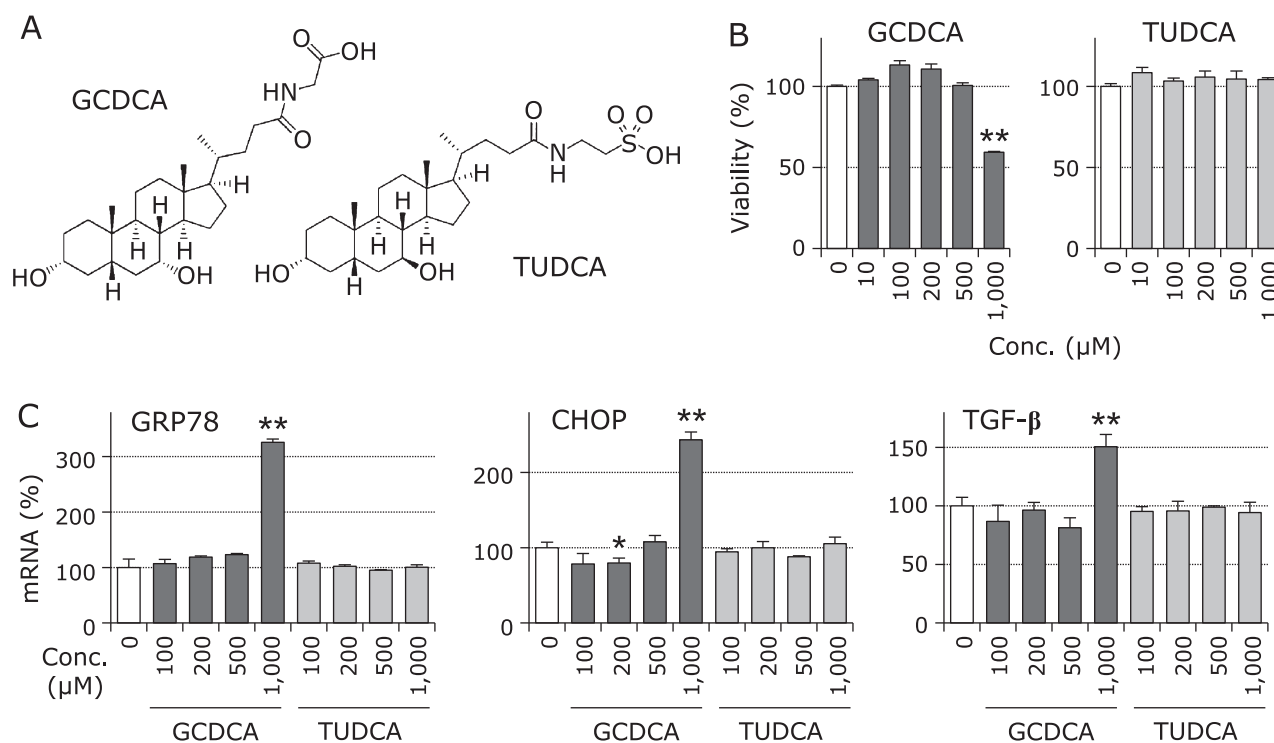


**Fig. 3.** Effects of GCDCA and TUDCA on HepG2 cell viability and the induction of ER stress. (A) Molecular structures of GCDCA and TUDCA. HepG2 cells were treated with the indicated concentrations of GCDCA and TUDCA for 24 h, followed by measurements of cell viability (B) and real-time PCR (C). Data are shown as the mean  $\pm$  SD ( $n = 3$ ). \* $p < 0.05$ , \*\* $p < 0.01$  vs vehicle.

assayed with an Apocycyto caspase-3 colorimetric assay kit (MBL, Nagoya, Japan) according to the manufacturer's directions.

**Detection of reactive oxygen species generation.** The cellular generation of reactive oxygen species (ROS) was quantified by the method described in our previous report<sup>(15)</sup> with minor modifications. After the treatment of HepG2 cells with CDCA, cells were washed once with PBS followed by incubation with fresh medium without serum containing 10  $\mu$ M 5-(and-6)-carboxy-2',7'-dichlorodihydrofluorescein diacetate (carboxy-H<sub>2</sub>DCFDA, Invitrogen) for 30 min under an atmosphere of 5% CO<sub>2</sub>/95% air at 37°C. After the incubation, cells were washed once with PBS and the fluorescence intensity of DCF was assayed (excitation, 485 nm; emission, 520 nm). Each fluorescence intensity was normalized relative to the cellular protein level in each

sample. DCF fluorescence-positive cells were visualized using an HS all-in-one fluorescence microscope BZ-9000 (Keyence, Tokyo, Japan).

**Assay of intracellular calcium.** HepG2 cells seeded in a 96-well culture plate were treated with CDCA. After the cells were washed once with PBS, intracellular Ca<sup>2+</sup> was monitored using Calcium kit-Fluo 4 (Dojindo, Kumamoto, Japan) according to the manufacturer's directions. Each fluorescence intensity was normalized relative to the cellular protein level in each sample.

**Data analysis.** Data are presented as the mean  $\pm$  SD from at least three experiments. Data were analyzed by the Mann-Whitney *U* test. A *p* value of less than 0.05 was considered significant.

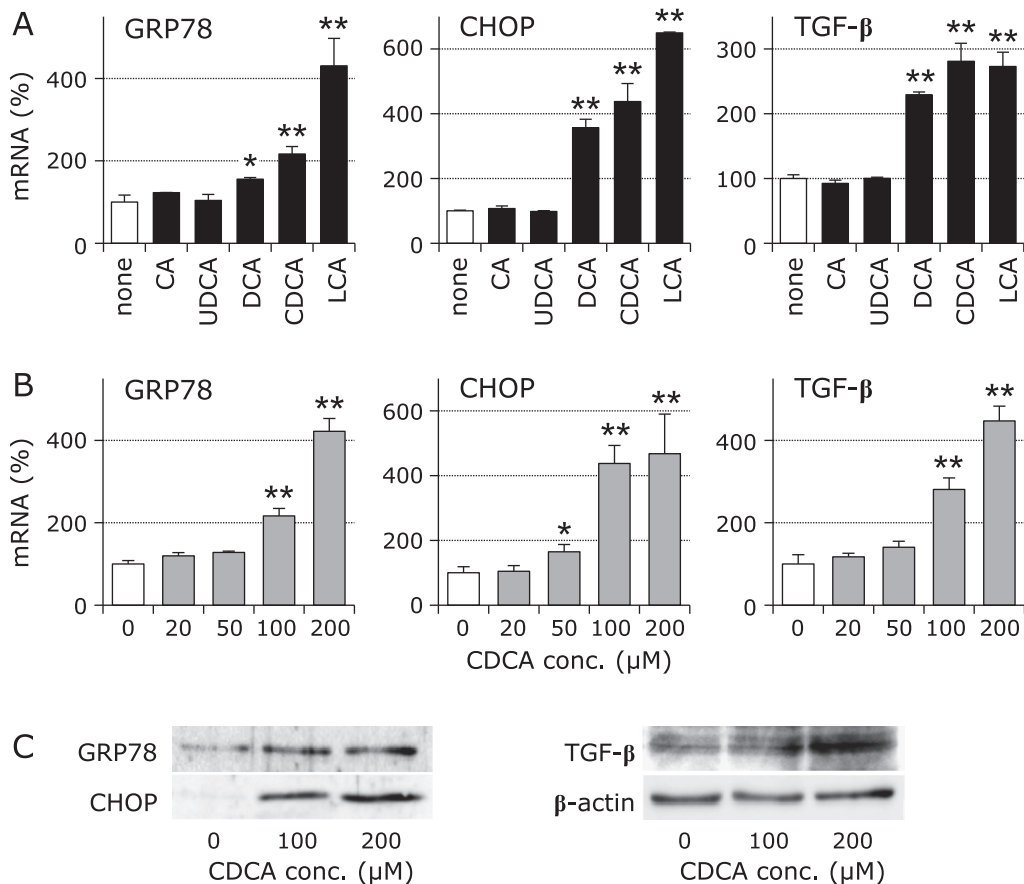


**Fig. 4.** Induction of ER stress and TGF- $\beta$  expression by unconjugated bile acids. (A) HepG2 cells were treated with 100  $\mu$ M unconjugated bile acids for 24 h, followed by real-time PCR. Data were normalized to GAPDH levels, and shown as the mean  $\pm$  SD ( $n = 3$ ). \* $p < 0.05$ , \*\* $p < 0.01$  vs vehicle (none). (B) HepG2 cells were treated with the indicated concentrations of CDCA for 24 h, followed by real-time PCR. Data are normalized to GAPDH levels, and shown as the mean  $\pm$  SD ( $n = 3$ ). \* $p < 0.05$ , \*\* $p < 0.01$  vs vehicle. (C) Western blotting analysis of HepG2 cells treated with the indicated concentrations of CDCA for 24 h.

## Results

### Effect of the various bile acids on HepG2 cell viability.

In order to determine the concentration and treatment time of the bile acids used in this study, we first measured HepG2 cell viability when these cells were treated with various concentrations and treatment times of CDCA because CDCA is the main component of plasma bile acids and exhibits moderate hydrophobicity. From the result that HepG2 cell viability was significantly suppressed by the treatment with 100  $\mu$ g/ml CDCA for 24 h, the cells were then treated with the other bile acids: CA, UDCA, DCA, and LCA, for 24 h, and their LD<sub>50</sub> were determined. The calculated LD<sub>50</sub> values of CA, UDCA, DCA, CDCA, and LCA were 882  $\mu$ M, 515  $\mu$ M, 171  $\mu$ M, 177  $\mu$ M, and 66  $\mu$ M, respectively, from the results shown in Fig. 2. Conjugated bile acids with either glycine or taurine, such as GCDCA or TUDCA, respectively, had lower hepatocyte toxicity than that of their unconjugated bile acids. In this experiment, GCDCA at 1 mM decreased HepG2 cell viability (Fig. 3B).

**Induction of ER stress and TGF- $\beta$  expression by the various bile acids.** The induction of ER stress in HepG2 cells by the various bile acids was determined. GRP78 and CHOP mRNA levels were significantly elevated by the relatively stronger hydrophobic bile acids, DCA, CDCA, and LCA, as shown in Fig. 4A. We confirmed, on behalf of the experimented bile acids, that these phenomena occurred in the concentration-dependent manner of CDCA (Fig. 4B). The activation of hepatocytes is known to be

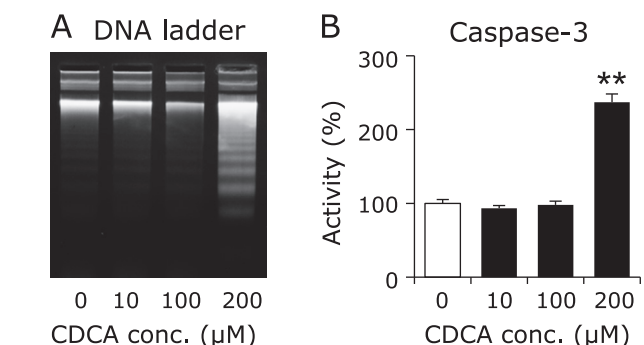


**Fig. 5.** Induction of apoptosis by CDCA. HepG2 cells were treated with the indicated concentrations of CDCA for 24 h, followed by the analysis of DNA fragmentation (A) and caspase-3 activity (B). \*\* $p < 0.01$  vs vehicle.

related to hepatic fibrosis. The expression of TGF- $\beta$  mRNA, a potent profibrogenic cytokine, was significantly elevated by hydrophobic bile acids and in a concentration-dependent manner (Fig. 4). The induction of these molecules by CDCA was also confirmed at the protein level (Fig. 4C).

The expression of GRP78, CHOP and TGF- $\beta$  mRNA was not induced by the relatively higher concentrations of GCDCA and TUDCA, except for 1 mM GCDCA again (Fig. 3C).

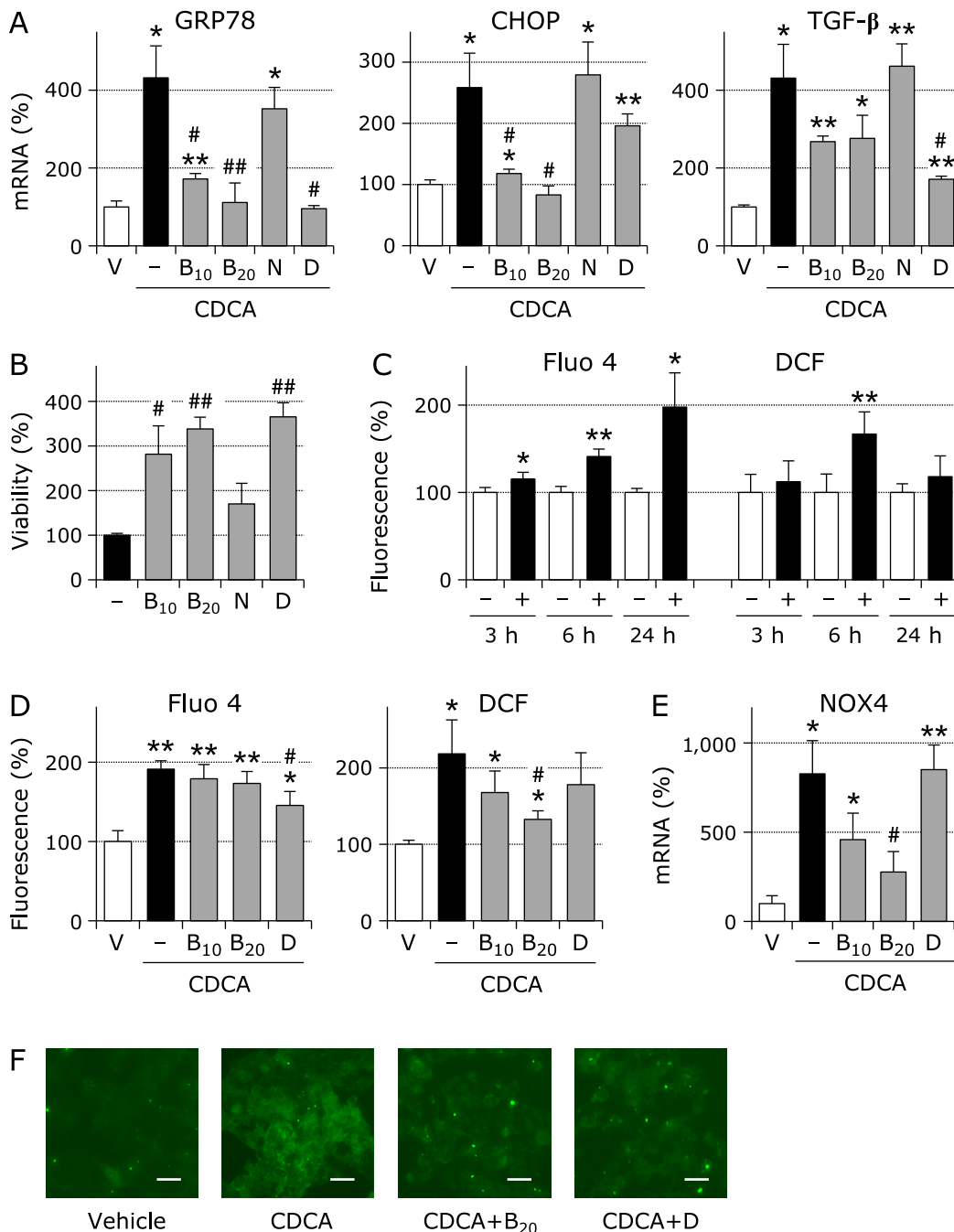


**Fig. 6.** Role of the increase in intracellular calcium and ROS generation. (A) HepG2 cells were treated with 200  $\mu$ M CDCA for 24 h with or without pretreatment (30 min) with BAPTA-AM (B<sub>10</sub>, 10  $\mu$ M; B<sub>20</sub>, 20  $\mu$ M), L-NAME (N, 1 mM), or DPI (D, 10  $\mu$ M), followed by real-time PCR. Data are normalized to GAPDH levels, and shown as the mean  $\pm$  SD ( $n = 3$ ). \* $p < 0.05$ , \*\* $p < 0.01$  vs vehicle (v). # $p < 0.05$ , ## $p < 0.01$  vs without an inhibitor (-). (B) HepG2 cells were treated with 300  $\mu$ M CDCA for 24 h with or without inhibitors, followed by measurements of cell viability with the MTT method. Data are shown as the mean  $\pm$  SD ( $n = 3$ ). \* $p < 0.05$ , \*\* $p < 0.01$  vs without an inhibitor (-). (C) HepG2 cells were treated with (+) or without (-) 200  $\mu$ M CDCA for the indicated hours, followed by measurements of intracellular Ca<sup>2+</sup> by the Fluo 4 fluorescence method and ROS generation by the DCF fluorescence method. \* $p < 0.05$ , \*\* $p < 0.01$  vs without CDCA. (D) HepG2 cells were treated with 200  $\mu$ M CDCA for 24 h (determination of intracellular Ca<sup>2+</sup>) or 6 h (determination of ROS) with or without BAPTA-AM or DPI, followed by fluorescence assays. Data are shown as the mean  $\pm$  SD ( $n = 3$ ). \* $p < 0.05$ , \*\* $p < 0.01$  vs vehicle (v). # $p < 0.05$ , \*\* $p < 0.01$  vs without an inhibitor (-). (E) HepG2 cells were treated with 200  $\mu$ M CDCA with or without inhibitors for 24 h, followed by RT-PCR for NOX4. Data are normalized to GAPDH levels, and shown as the mean  $\pm$  SD ( $n = 3$ ). \* $p < 0.05$ , \*\* $p < 0.01$  vs vehicle. # $p < 0.05$  vs without an inhibitor (-). (F) Intracellular ROS generation by CDCA was observed using a HS all-in-one fluorescence microscope BZ-9000. HepG2 cells were treated with 200  $\mu$ M CDCA for 6 h with or without BAPTA-AM or DPI, and then visualized with DCF fluorescence dye. Scale bar shows 50  $\mu$ m.

**Bile acid-induced apoptosis.** Treatment with CDCA induced DNA fragmentation and elevations in caspase-3 activity as the signals of apoptosis, as shown in Fig. 5.

**Changes in intracellular calcium levels and the generation of reactive oxygen species.** Bile acid-induced cell death has been associated with an enhancement in the generation of ROS

and reactive nitrogen species.<sup>(16,17)</sup> ER stress and oxidative stress are known to be related to calcium signaling disturbances.<sup>(18)</sup> We investigated the role of intracellular calcium in the CDCA-induced up-regulation of ER stress markers using the highly specific intracellular calcium chelator BAPTA. The addition of BAPTA-AM significantly suppressed the effect of CDCA on the mRNA levels of GRP78 and CHOP. The induction of TGF- $\beta$  by CDCA was also moderately suppressed by BAPTA-AM. DPI is an inhibitor of NADPH oxidase (NOX), a major intracellular ROS-generating enzyme. The addition of DPI also significantly suppressed the up-regulation of GRP78 and TGF- $\beta$ , while the nitric oxide synthase inhibitor, L-NAME did not, as shown in Fig. 6A. A reduction in cell viability due to the CDCA treatment was suppressed by BAPTA and DPI, but not by L-NAME (Fig. 6B).

Changes in intracellular Ca<sup>2+</sup> levels and ROS generation by CDCA were determined with the specific fluorescence probes, Fluo 4 AM and carboxy-H<sub>2</sub>DCFDA, respectively. A maximal increase in ROS generation was detected when HepG2 cells were treated with CDCA for 6 h, whereas intracellular Ca<sup>2+</sup> levels increased in a time-dependent manner (Fig. 6C). The increase in intracellular Ca<sup>2+</sup> levels was significantly suppressed by the pretreatment with DPI, while the generation of ROS was significantly suppressed by BAPTA, as shown in Fig. 6D. The expression of NOX4, a NOX isoform, in HepG2 cells was markedly induced by the treatment with CDCA and this was significantly suppressed by BAPTA, as shown in Fig. 6E. Intracellular ROS generation in HepG2 cells by CDCA and its suppression with inhibitors were observed with the fluorescent dye (Fig. 6F).

## Discussion

Cholestasis is a cause of liver fibrosis, and hepatocyte death is a key initiator that triggers a hepatic fibrotic response. However, although the mechanism of bile acid toxicity on hepatocyte death is not fully understood, its hydrophobicity has been believed to be an important cytotoxicity determinant of bile acids.<sup>(13,19)</sup> The results shown in Figs. 2, 3 and 4 suggest that the intensities of cytotoxicity and ER stress induced by the bile acids tested were generally dependent on their hydrophobicity because the results correlated well with the known order for the magnitude of hydrophobicity (lipophilicity) in these bile acids; CA < UDCA < DCA  $\approx$  CDCA < LCA.<sup>(13)</sup> This is roughly in accordance with numerous previous studies.<sup>(19,20)</sup> These observations were also consistent with a previous report, which showed that CA, UDCA and DCA were not cytotoxic in human vascular endothelial cells.<sup>(21)</sup> The most hydrophobic bile acid LCA was not detected in the sera of either healthy subjects or liver cirrhosis patients.<sup>(8)</sup> The serum concentrations of total bile acid, CDCA, UDCA and CA were markedly higher in patients with hepatobiliary diseases than in healthy subjects. Among these bile acids, CDCA, both free acid and its conjugates, was particularly increased.<sup>(8)</sup> Serum DCA concentrations were shown to be markedly lower than those of the above bile acids in both healthy subjects and patients.<sup>(8)</sup> GCDCA and TUDCA had relatively lower hydrophobicity with R<sub>MW</sub> values of 2.92 and 1.71, respectively.<sup>(13)</sup> GCDCA triggered ER stress and cell death only at concentrations up to 1 mM. From these results, the unconjugated form of CDCA may actually cause pathological conditions as toxic bile acid in hepatobiliary diseases.

Hepatocytes are rich in ER. Because of their high protein synthesizing capacity, it is easy to speculate that the ER stress response may play an important role in mediating pathological changes in liver diseases.<sup>(4)</sup> When activation of the UPR fails to promote cell survival, in spite of the displacement of GRP78 from the stress sensor to aid in protein folding and restoration of the homeostatic balance, the cell is broken down by the proapoptotic ER stress response pathway. An important and frequent feature of the ER stress response is the increased expression of CHOP, which has been shown to activate the proapoptotic pathway.<sup>(22)</sup>

Caspase is a member of the cysteine/aspartic acid-specific protease family, which is activated by various signals and plays pivotal roles in the apoptotic process, and caspase-3 is a convergence point of various apoptosis-regulating signal pathways.<sup>(23)</sup> We observed the activation of caspase-3 and DNA fragmentation by the CDCA treatment, which confirmed the contribution of apoptosis.

Previous reports have shown that the application of bile acids can cause an increase in cytosolic Ca<sup>2+</sup> levels in hepatocytes and other cells,<sup>(24,25)</sup> resulting in Ca<sup>2+</sup>-dependent apoptosis.<sup>(25)</sup> A major part of Ca<sup>2+</sup> released into the cytosol is recruited from the ER,<sup>(25,26)</sup> and the disruption of ER Ca<sup>2+</sup> homeostasis triggers ER stress because the depletion of Ca<sup>2+</sup> in the ER can stagnate protein folding and transport.<sup>(26)</sup> Moreover, an overload of cytosolic Ca<sup>2+</sup> has been shown to initiate ROS generation by mitochondria<sup>(27)</sup> and NOX.<sup>(28)</sup> In this study, we demonstrated that BAPTA significantly inhibited the up-regulation of ER stress markers and NOX4 and ROS production induced by CDCA, as shown in Fig. 6.

A crosstalk between the generation of ROS and the ER stress response has been indicated in previous studies<sup>(29)</sup> because the redox status within the lumen of the ER affects protein folding and disulfide formation. Alterations in disulfide bond formation or the mispairing of cysteine residues was shown to result in the aggregation or accumulation of misfolded proteins and/or protein dysfunction in the ER lumen.<sup>(30)</sup> ER stress has been shown to increase ROS formation because the accumulation of unfolded and misfolded proteins in the ER triggers Ca<sup>2+</sup> leakage into the cytosol and stimulates intracellular ROS production.<sup>(30)</sup> NOX4, one of the NOX isoforms implicated as a possible ROS source during pathological conditions, was shown to be induced by oxysterols and mediated ER stress.<sup>(31)</sup> We demonstrated that CDCA markedly induced NOX4, as shown in Fig. 6E. Moreover, the NOX4 inhibitor DPI significantly suppressed the up-regulation of ER stress markers, elevation in intracellular Ca<sup>2+</sup> levels, and decline in cellular viability. Excessive ROS are known to raise the cytosolic Ca<sup>2+</sup> concentration, which subsequently cause the generation of new ROS.<sup>(32)</sup> The results from the present study clearly showed that ROS generation by NOX4 and the elevation in intracellular Ca<sup>2+</sup> synergistically stimulated the progression of CDCA-induced ER stress and cellular injury. This finding is consistent with that from an *in vivo* study, which showed a good correlation between hepatic bile acid concentrations and hepatic oxidative stress marker levels.<sup>(16)</sup>

TGF- $\beta$  is a potent profibrogenic factor that stimulates the trans-differentiation and proliferation of hepatic stellate cells, expression of the matrix, hepatocyte apoptosis, and ultimately liver fibrosis.<sup>(33)</sup> A previous study showed that liver fibrosis-induced bile duct ligation was attenuated in CHOP-knockout mice accompanied by the suppression of TGF- $\beta$ .<sup>(34)</sup> Our results are consistent with the above findings and indicate that the ER stress pathway plays an essential role in bile acid-induced hepatocyte injury.

Chronic cholestasis occurs in diseases such as biliary atresia and sclerosing cholangitis, and causes liver fibrosis, which eventually leads to cirrhosis. In conclusion, our study demonstrated that bile acids induced ER stress via an elevation in intracellular Ca<sup>2+</sup> and/or ROS generation, which in turn stimulated apoptosis, in a hydrophobicity-dependent manner. These results have potential implications for the pathogenesis of cholestatic liver diseases in which ER stress participates in hepatocellular injury.

## Acknowledgments

This study was supported in part by a Grant-in-Aid for Scientific Research from the Japan Society for the Promotion of Science (to T.A., No. 21590169).

## Abbreviations

BAPTA	1,2-bis(2-aminophenoxy)ethane- <i>N,N,N',N'</i> -tetraacetic acid tetraacetoxymethyl ester
CA	cholic acid
Carboxy-H <sub>2</sub> DCFDA	5-(and-6)-carboxy-2',7'-dichlorodihydrofluorescein diacetate
CDCA	chenodeoxycholic acid
CHOP	C/EBP homologous protein
DCA	deoxycholic acid
DPI	diphenyleneiodonium
ER	endoplasmic reticulum
GAPDH	glyceraldehyde-3-phosphate dehydrogenase
GCDCa	glycochenodeoxycholic acid

GRP78	glucose-regulated protein 78
LCA	lithocholic acid
L-NAME	<i>N</i> <sup>G</sup> -nitro-L-arginine methyl ester
MTT	3-(4,5-di-methylthiazol-2-yl)-2,5-diphenyltetrazolium bromide
ROS	reactive oxygen species
TGF-β	transforming growth factor-β
TUDCA	tauroursodeoxycholic acid
UDCA	ursodeoxycholic acid
UPR	unfolded protein response

## Conflict of Interest

No potential conflicts of interest were disclosed.

## References

- Zhang Y, Limaye PB, Lehman-McKeeman LD, Klaassen CD. Dysfunction of organic anion transporting polypeptide 1a1 alters intestinal bacteria and bile acid metabolism in mice. *PLoS One* 2012; **7**: e34522.
- Ridlon JM, Kang DJ, Hylemon PB. Bile salt biotransformations by human intestinal bacteria. *J Lipid Res* 2006; **47**: 241–259.
- Yoshida H. ER stress and diseases. *FEBS J* 2007; **274**: 630–658.
- Dara L, Ji C, Kaplowitz N. The contribution of endoplasmic reticulum stress to liver disease. *Hepatology* 2011; **53**: 1752–1763.
- Bertolotti A, Zhang Y, Hendershot LM, Harding HP, Ron D. Dynamic interaction of BiP and ER stress transducers in the unfolded-protein response. *Nat Cell Biol* 2000; **2**: 326–332.
- Marciniak SJ, Yun CY, Oyadomari S, et al. CHOP induces death by promoting protein synthesis and oxidation in the stressed endoplasmic reticulum. *Genes Dev* 2004; **18**: 3066–3077.
- Nakajima T, Okuda Y, Chisaki K, et al. Bile acids increase intracellular Ca<sup>2+</sup> concentration and nitric oxide production in vascular endothelial cells. *Br J Pharmacol* 2000; **130**: 1457–1467.
- Chisaki K, Nakajima T, Iwasawa K, et al. Enhancement of endothelial nitric oxide production by chenodeoxycholic acids in patients with hepatobiliary diseases. *Jpn Heart J* 2001; **42**: 339–353.
- Li MK, Crawford JM. The pathology of cholestasis. *Semin Liver Dis* 2004; **24**: 21–42.
- Ramadori G, Saile B. Portal tract fibrogenesis in the liver. *Lab Invest* 2004; **84**: 153–159.
- Sagawa H, Tazuma S, Kajiyama G. Protection against hydrophobic bile salt-induced cell membrane damage by liposomes and hydrophilic bile salts. *Am J Physiol* 1993; **264**: G835–G839.
- Powell AA, Larue JM, Batta AK, Martinez JD. Bile acid hydrophobicity is correlated with induction of apoptosis and/or growth arrest in HCT116 cells. *Biochem J* 2001; **356**: 481–486.
- Sharma R, Majer F, Peta VK, et al. Bile acid toxicity structure-activity relationships: correlations between cell viability and lipophilicity in a panel of new and known bile acids using an oesophageal cell line (HET-1A). *Bioorg Med Chem* 2010; **18**: 6886–6895.
- Kamiya T, Hara H, Yamada H, Imai H, Inagaki N, Adachi T. Cobalt chloride decreases EC-SOD expression through intracellular ROS generation and p38-MAPK pathways in COS7 cells. *Free Radical Res* 2008; **42**: 949–956.
- Adachi T, Aida K, Nishihara H, Kamiya T, Hara H. Effect of hypoxia mimetic cobalt chloride on the expression of extracellular-superoxide dismutase in retinal pericytes. *Biol Pharm Bull* 2011; **34**: 1297–1300.
- Nomoto M, Miyata M, Yin S, et al. Bile acid-induced elevated oxidative stress in the absence of farnesoid X receptor. *Biol Pharm Bull* 2009; **32**: 172–178.
- Leindler L, Morschl E, László F, et al. Importance of cytokines, nitric oxide, and apoptosis in the pathological process of necrotizing pancreatitis in rats. *Pancreas* 2004; **29**: 157–161.
- González-Rubio S, Linares CI, Bello RI, et al. Calcium-dependent nitric oxide production is involved in the cytoprotective properties of n-acetylcysteine in glycochenodeoxycholic acid-induced cell death in hepatocytes. *Toxicol Appl Pharmacol* 2010; **242**: 165–172.
- Heuman DM. Quantitative estimation of the hydrophilic-hydrophobic balance of mixed bile salt solutions. *J Lipid Res* 1989; **30**: 719–730.
- Perez MJ, Briz O. Bile-acid-induced cell injury and protection. *World J Gastroenterol* 2009; **15**: 1677–1689.
- Garner CM, Mills CO, Elias E, Neuberger JM. The effect of bile salts on human vascular endothelial cells. *Biochim Biophys Acta* 1991; **1091**: 41–45.
- Ohoka N, Yoshii S, Hattori T, Onozaki K, Hayashi H. TRB3, a novel ER stress-inducible gene, is induced via ATF4-CHOP pathway and is involved in cell death. *EMBO J* 2005; **24**: 1243–1255.
- Zou W, Zeng J, Zhuo M, et al. Involvement of caspase-3 and p38 mitogen-activated protein kinase in cobalt chloride-induced apoptosis in PC12 cells. *J Neurosci Res* 2002; **67**: 837–843.
- Gerasimenko JV, Flowerdew SE, Voronina SG, et al. Bile acids induce Ca<sup>2+</sup> release from both the endoplasmic reticulum and acidic intracellular calcium stores through activation of inositol trisphosphate receptors and ryanodine receptors. *J Biol Chem* 2006; **281**: 40154–40163.
- Criddle DN, Gerasimenko JV, Baumgartner HK, et al. Calcium signalling and pancreatic cell death: apoptosis or necrosis? *Cell Death Differ* 2007; **14**: 1285–1294.
- Concannon CG, Ward MW, Bonner HP, et al. NMDA receptor-mediated excitotoxic neuronal apoptosis *in vitro* and *in vivo* occurs in an ER stress and PUMA independent manner. *J Neurochem* 2008; **105**: 891–903.
- Duan Y, Gross RA, Sheu SS. Ca<sup>2+</sup>-dependent generation of mitochondrial reactive oxygen species serves as a signal for poly(ADP-ribose) polymerase-1 activation during glutamate excitotoxicity. *J Physiol* 2007; **585**: 741–758.
- Kim TH, Kim Js, Kim Zh, Huang RB, Wang RS. Khz (fusion of *Ganoderma lucidum* and *Polyporus umbellatus* mycelia) induces apoptosis by increasing intracellular calcium levels and activating JNK and NADPH oxidase-dependent generation of reactive oxygen species. *PLoS One* 2012; **7**: e46208.
- Bhandary B, Marahatta A, Kim HR, Chae HJ. An involvement of oxidative stress in endoplasmic reticulum stress and its associated diseases. *Int J Mol Sci* 2012; **14**: 434–456.
- van der Vlies D, Makkinje M, Jansens A, et al. Oxidation of ER resident proteins upon oxidative stress: effects of altering cellular redox/antioxidant status and implications for protein maturation. *Antioxid Redox Signal* 2003; **5**: 381–387.
- Pedruzzi E, Guichard C, Ollivier V, et al. NAD(P)H oxidase Nox-4 mediates 7-ketocholesterol-induced endoplasmic reticulum stress and apoptosis in human aortic smooth muscle cells. *Mol Cell Biol* 2004; **24**: 10703–10717.
- Jiang CP, Ding H, Shi DH, Wang YR, Li EG, Wu JH. Pro-apoptotic effects of tectorigenin on human hepatocellular carcinoma HepG2 cells. *World J Gastroenterol* 2012; **18**: 1753–1764.
- Gressner AM, Weiskirchen R. Modern pathogenetic concepts of liver fibrosis suggest stellate cells and TGF-β as major players and therapeutic targets. *J Cell Mol Med* 2006; **10**: 76–99.
- Tamaki N, Hatano E, Taura K, et al. CHOP deficiency attenuates cholestasis-induced liver fibrosis by reduction of hepatocyte injury. *Am J Physiol Gastrointest Liver Physiol* 2008; **294**: G498–G505.